Scale Effects in Rock Masses, Pinto da Cunha (ed.) © 1990 Balkema, Rotterdam. ISBN 90 6191 126 5

Roughness scale effects and fractal dimension

N. H. Maerz & J. A. Franklin
University of Waterloo, Ont., Canada

ABSTRACT: Using shadow profilometry, the authors have investigated the effect of the scale of observation on measurements of roughness, and have confirmed that a roughness scale effect exists. The method of measurement acts as a bandpass filter, allowing scale effects to be quantified from images at different magnifications.

Fractal dimension has also been investigated as a means of characterizing roughness. The rock profiles tested were found not to be self-similar at different scales of observation, providing further evidence for a scale effect.

1 INTRODUCTION

From the measured roughness of a rock joint can be predicted shear strength (Patton, 1966; Ladanyi and Archambault, 1969; Barton, 1973), hydraulic conductivity (Barton et al., 1985; Elsworth and Goodman, 1986), and deformability (Swan, 1983; Bandis et al. 1983).

Methods for measuring roughness, such as electro-mechanical profilometers, are usually impractical, slow and complicated. Data collection often presents excessive risk to personnel, and the amount and quality of data collected are usually inadequate for valid statistical representation. Shadow profilometry (Maerz et al., 1990) is an alternative and simpler tool. It relies on the principle of the Schmaltz microscope (Schmaltz, 1936) which produces a profile of a surface by projecting a linear shadow edge onto a roughness surface (Fig. 1). The undulating shadow is photographed, digitized, and processed to isolate the roughness waveform, which is then characterized by measuring one of many available geometrical or statistical parameters.

A roughness parameter employed in this paper is the "micro-average i-angle", a measure of the slope of the digital trace equal to the average angle between the mean plane of roughness and adjacent pixels on the digital waveform. The waveform is sampled at an interval called the "resolution" of the image, which in the author's image analyzing system is equal to the pixel separation.

2 ROUGHNESS SCALE EFFECTS

2.1 Introduction

A scale effect exists if measurements of the same surface at different scales of observation give different roughness values. From previous studies using shadow profilometry, we had observed that increased sampling lengths tended to give reduced values of slope-type roughness parameters. The same was reported by Barton and Choubey (1977), who found that asperities of long wavelength tend to be less steep.

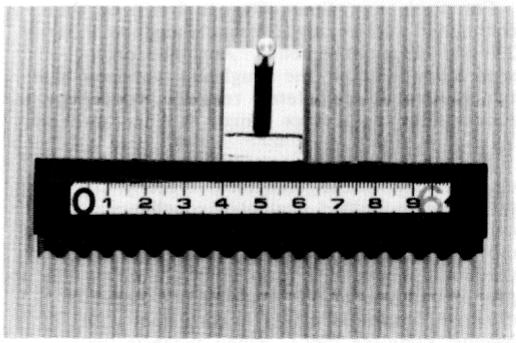

Fig. 1: Shadow cast on corrugated cardboard.

2.2 Tests on corrugated cardboard

To test the profilometry method itself, images were analyzed of corrugated cardboard with wave amplitude of 2.5 mm and wavelength of 6.5 mm. If the method returned similar values of roughness irrespective of the scale of observation, this would demonstrate freedom from inherent scale effects.

Profiles were digitized at trace lengths of 20, 50, 100, 200, 500, and 1000 mm (Fig. 2), corresponding to pixel separations (i-angle base lengths) of about 0.04, 0.1, 0.2, 0.4, 1, and 2 mm respectively. The

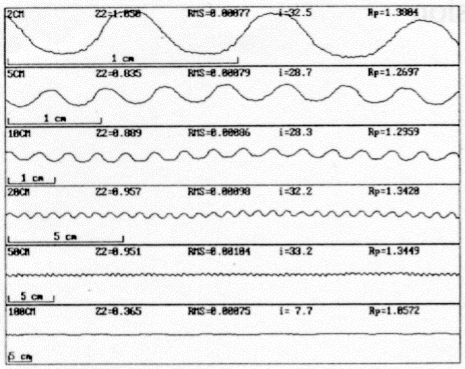

Fig. 2: Profiles of corrugated cardboard at different scales of observation.

pixel separation defines the resolution of the image, and depends on the distance from the camera to the rock surface (called the object distance).

The resulting profiles showed a well-defined sinusoidal waveform at up to 200 mm trace length (0.4 mm pixel separation). At 500 mm trace length (1 mm pixel separation), the sinusoidal shape was compromised by lack of resolution. At 1000 mm trace length (2 mm pixel separation), the waveform was almost completely lost because of poor resolution. Also evident at extremes of scale were a higher frequency (roughness of the paper itself) and a lower frequency (undulation of the mean plane of the paper).

For pixel separations of up to 1 mm on the corrugated surface, the average i-angle was 31° ± 2.7° for all measurements. At 2 mm pixel separation however, the roughness waveform was too small to be completely resolved, so the measured micro-average i-angle was far lower at 7.7°.

The experiment demonstrated that for a characteristic size of roughness asperity, the profilometry method evaluated roughness consistently until the asperity size approached the effective resolution of the system. For the cardboard example, a ratio of height of asperity to pixel separation of 2.5:1 marked the limits of effective resolution. This is consistent with Nyquist sampling theory which suggests that frequencies greater than twice the sampling rate will not be resolved.

This is nothing more than a low pass filtering effect. Similarly, a high pass filtering occurs if a complete wavelength is not sampled. These two limiting effects combine to make the sampling procedure a bandpass filter.

2.3 Tests on rock joint surfaces

The roughness asperities on a rock joint surface are not of a single characteristic size, but include multiple superpositions of different sizes. Because the sampling procedure acts as a bandpass filter, only those wavelengths that can be effectively sampled will contribute to the measured roughness.

Two series of field tests were conducted to investigate scale effect. In the first, three profiles each at 100, 200, 500, and 1000 mm trace lengths were taken in the INCO Creighton Mine, Sudbury Canada, using shadow profilometry. In the second test series, a 5 m vertical joint face on a road cut 100 km south of Sudbury was used. A surveyors chord, marked off in 200 mm intervals, was stretched out horizontally. One measurement was taken of the entire 5 m length, two at 2 m lengths, six at 0.8 m lengths, twelve at 0.4 m lengths, and twenty-one at 0.2 m lengths. A typical profile of each trace is shown in Fig. 3. For these profiles, the pixel separations were equivalent to about 10, 4, 1.6, 0.8, and 0.4 mm measured on the rock surface.

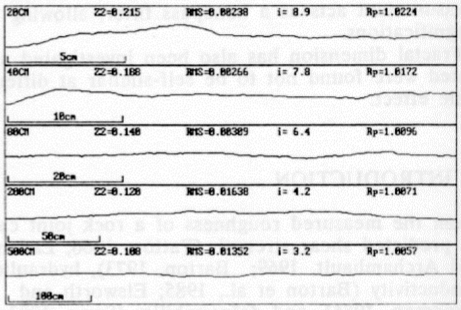

Fig. 3: Profiles of a rock joint at different scales of observation.

The road cut experiment results are given in Fig. 4. In this and also in the Creighton Mine experiment, measured roughness was found to decrease non-linearly as the pixel separation increased. This scale effect results from a change in pixel separation for images at different object distances. By changing the object distance, the i-angle (from pixel to pixel) is measured over a range of base lengths.

The same scale effect could be determined from a single image by measuring the gradients of lines joining every second, third etc. pixel, although the range of investigation would then be limited by the bandpass filter for the given single image.

The scale effect found in these experiments is a true characteristic of the rock surface, although measured by a technique that makes use of a method-dependent image resolution. Pixel-to-pixel gradient implies measurement at a specific scale. Micro-average i-angle therefore must be represented as a curve or graph as in Fig. 4, not as a single value. The curve could be characterized by parameters of a curvilinear equation. There may be other measures of roughness that are scale invariant.

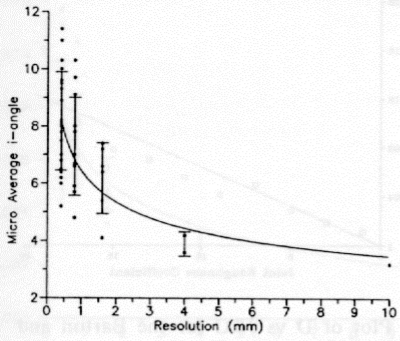

Fig. 4: Micro-average i-angles of Fig. 3 profiles, as a function of trace length, with power law best fit. Error bars are standard deviations.

3 FRACTAL DIMENSION

3.1 Introduction

The concept of a fractal dimension was introduced to resolve an enigma in the measurement of the length of irregular objects such as coastlines (Mandelbrot, 1982). Conceptually, the length of an undulating coastline is not a constant, but depends on the length of the measuring "yardstick". When measured with a long yardstick, a coastline appears shorter than when measured with a short one.

In the Mandelbrot Richardson covering method (Mandelbrot 1982), the fractal dimension of the coastline can be calculated by counting the number (n) of yardsticks of length r that are needed to cover the extent of the profile. This measurement is repeated for various lengths of r. Finally, log (r) is plotted against log (nr).

According to Mandelbrot, if this plot is linear, the coastline is a "fractal object" and the slope can be equated to 1-D where D is the fractal dimension. The magnitude D is a function of roughness; the more undulating the object, the higher the fractal dimension. It has a minimum value of 1.0 for a straight line and approaches 2.0 for an extremely rough line.

For the fractal dimension to be constant (i.e. a linear slope on the plot) the object must be self-similar, meaning that its form is the same at all scales of observation. If the object is not self similar (not fractal), then D is not a constant but rather a function of the scale of observation.

Fractal analysis of this type has been applied to rock surfaces by Zipf and Bieniawski (1988), Carr and Wariner (1987), Turk et al. (1987), and Barton and Larson (1985); to metal fractures by Banerji and Underwood (1983) and Chernant and Coster (1978); to microstructures by Farin et al. (1985), Pfeifer (1983), and Wright and Karlsson (1982); and to fault systems by Aviles and Scholz (1987), and Okubo and Aki (1987).

There are, however, reasons why fractal analysis may not be appropriate for characterizing the roughness of rock joint surfaces:

- Mandelbrot (1985) suggests that relief profiles are not self-similar. Although the fractal dimension of non-fractal objects can always be calculated, it has no theoretical meaning.

- The fractal dimension of a continuous differentiable function such as a sine wave is 1 (Mandelbrot 1982), the same as that of a straight line. From a rock mechanics viewpoint a sinusoidal surface and a flat surface have very different roughnesses, which should be reflected in the measured values.

3.2 Verification of the fractal dimension method

An algorithm was developed which used the Mandelbrot-Richardson covering method to calculate the fractal dimension D of a digitized profile. The values of log (r) vs. log (nr) were plotted, and a linear least squares best fit was calculated.

The method was verified by measuring D for three different objects whose dimension is known; a straight line, a von Koch snowflake (Fig. 5), and a sinusoidal wave.

As expected, the measured D of the straight line was 1.00. For the von Koch snowflake, the measured D of 1.214 proved less than the theoretical value of D = (log 4)/(log 3) = 1.262 (Voss, 1988). This is attributed to the resolution limitations of the image analysis system.

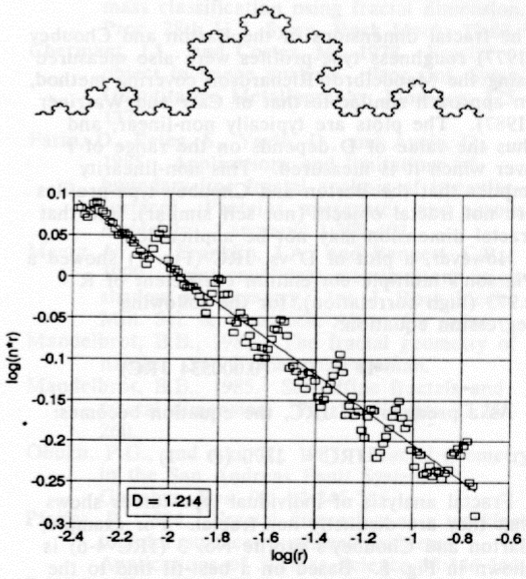

Fig. 5: The Von Koch snowflake: (a) configuration of the snowflake, a fractal object with D = 1.262 (b) Linear fractal plot of the Von Koch snowflake showing a measured D of 1.214.

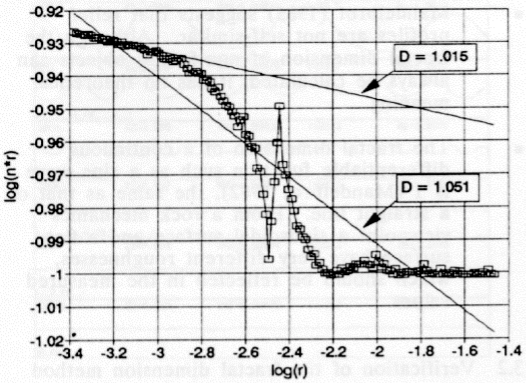

Fig. 6: Fractal plot of a sine wave. The non-linear fractal dimension depends on the range over which it is calculated.

The sine wave was analyzed as an example of a continuous differentiable function whose D should be 1. The resulting fractal plot (Fig. 6) was severely non-linear with D = 1.051 as an "average" for the data as a whole. However, when determined at small r (smallest possible under the constraints of the image analysis system), the D reduced to 1.015. At very small r, D may approach 1.0.

3.3 Correlation of fractal dimension with JRC

The fractal dimensions of the Barton and Choubey (1977) roughness type-profiles were also measured using the Mandelbrot Richardson covering method, an approach similar to that of Carr and Warriner (1987). The plots are typically non-linear, and thus the value of D depends on the range of r over which it is measured. This non-linearity implies that the Barton and Choubey type-profiles are not fractal objects (not self similar), and that fractal dimension may not be applicable.

However, a plot of D vs. JRC (Fig. 7) showed a Pierson's multiple correlation coefficient of R = 0.973 (high correlation), for the following regression equation:

$$D = 1 + (0.000534\ JRC)$$

As a predictor of JRC, the equation becomes:

$$JRC = 1870\ (D - 1)$$

Fractal analysis of individual type-curves shows that they are distinctly non-fractal. For example, Barton and Choubey's profile No. 3 (JRC 4-6) is shown in Fig. 8. Based on a best-fit line to the entire curve, D = 1.00286, equivalent to JRC = 5.3 using the above linear predictive equation. However, if D is calculated using only the right or left extremes of the graph, it varies from 1.00071 to 1.00696, equivalent to a JRC range of 1.3 to 13.0. This reveals a scale effect, and underlines

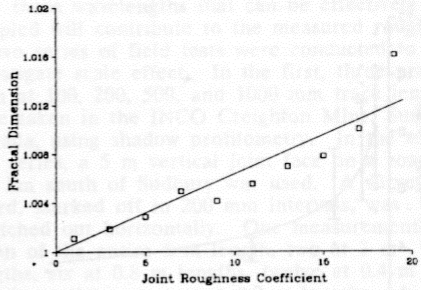

Fig. 7: Plot of D vs JRC for the Barton and Choubey (1977) type profiles.

the danger of applying fractal analysis indiscriminately to non-fractal objects.

3.4 Fractal dimension of rock joint surfaces

Fractal dimension was estimated for the rock joint profiles described in Section 2.3, using the Mandelbrot-Richardson covering method. The fractal plots were found to be non-linear indicating that the rock surface was non-fractal.

In a further experiment, the fractal dimension was measured by changing the resolution, a method proposed by Chernant and Coster (1978). This made use of the profiles with trace lengths of 200, 400, 800, 2000, and 5000 mm and resolutions of 0.4, 0.8, 1.6, 4, and 10 mm respectively. Values of r were scaled relative to the resolution.

A self-similar (fractal) surface should have identical D for all resolutions. Figure 9 shows that the measured D in fact increased with increasing resolution, confirming a non-fractal rock surface. There is an obvious scale effect. In fact, this graph looks remarkably like Figure 5,

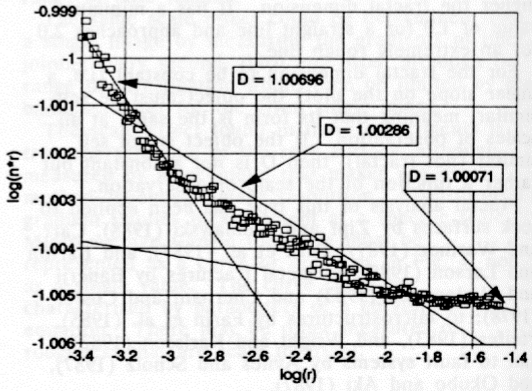

Fig. 8: Fractal plot of Barton and Choubey (1977) profile No. 3 (JRC = 4-6).

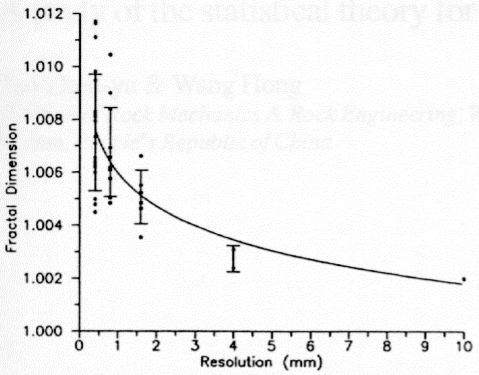

Fig. 9: Fractal dimension measurement of the profiles of Fig. 3 as a function of base length, with power law best fit. Error bars are sample standard deviations.

indicating that fractal dimension is no more scale independent than a simple slope type index parameter, such as i-angle.

4 Discussion and conclusions

Shadow profilometry has been used to demonstrate a roughness scale effect on rock joint surfaces. The shorter the base length over which the i-angle is measured, the steeper the average asperity angle.

Similarly, the measured rock joint surfaces have been shown to be non-fractal. Their fractal plots are non-linear, and D decreases for longer "yardsticks", which gives further confirmation of a roughness scale effect.

Although D is highly correlated with JRC for the Barton and Choubey type-profiles, JRC can be predicted only if D is calculated from a straight line fitted to the same range of 'r' values as used to derive the correlation equation. The data set is decidedly curved, and scale effects can lead to considerable errors in estimating JRC.

Some authors have suggested that the fractal approach is valid if the fractal plot is piecewise linear (Barton and Larson, 1985). Theoretically, the fractal dimension of an object is taken at the limit as the length of the "yardstick" approaches zero (Voss, 1988). The resolution constraints of any measuring system, however, dictate a finite lower limit for the length of the "yardstick", at or near the limit of resolution, e.g. the pixel size. Resolution limitations can be overcome to the extent required, by close-up photography combined with mosaicing to examine long wavelengths.

Note that long wavelengths may be at least as important as short ones in governing properties such as shear strength. Therefore parameters that characterize roughness only over a narrow range of wavelengths (small, for example), may turn out to be poor predictors of shear strength. Roughness should be measured at all wavelengths, small and large, and characterized by parameters that define a size-roughness curve.

A further flaw in the use of fractal dimension is that identical values of D are given to a sine curve and a straight line. This is intuitively unacceptable in rock mechanics applications.

Acknowledgements

The authors would like to thank Dr. E. R. Vrscay of the Dept. of Applied Mathematics, University of Waterloo, for his help with Fractal Analysis, and also the Centre de Téchnologie Noranda for their support for the development of the shadow profilometry method.

REFERENCES

Aviles, C.A., and Scholz, C.H., 1987. Fractal analysis applied to characteristic segments of the San Andreas Fault. J. Geophysical Research 92, b1:331-334.

Banerji, K., and Underwood, E.E., 1983. Quantitative analysis of fractographic features in a 4340 steel. Acta Sterol. 2, Suppl. I:65-70.

Barton, C.C., and Larsen, E., 1985. Fractal geometry of two dimensional fracture networks at Yucca Mountain, southwest Nevada. Proc. Int. Symp. on Fundamentals of Rock Joints, Björkliden: 77-84.

Barton N., and Choubey V., 1977. The shear strength of rock joints in theory and in practice. Rock Mechanics 10:1-54.

Carr, J.R., and Warriner, James B., 1987. Rock mass classification using fractal dimension. Proc. 28th U.S. Symp. Rock Mech: 73-80.

Chermant, J.L., and Coster, M., 1978. Fractal object in image analysis. Proc. Int. Symp. Quantitative Metallography, Florence: 125-137.

Farin, D., Peleg, S., Yavin, D., and Avnir, D., 1985. Applications and limitations of boundary line fractal analysis of irregular surfaces. Proteins, aggregates, and porous materials. Langmuir 1:399-407.

Maerz, N. H., Franklin, J.A., and Bennett, C.P., 1990. Joint roughness measurement using shadow profilometry. Int. J. Rock Mech. Min. Sci. & Geomech. Abstr. (in press)

Mandelbrot, B.B., 1982. The fractal geometry of nature. San Francisco: Freeman.

Mandelbrot, B.B., 1985. Self-affine fractals and fractal dimension. Physica Scripta 32:257-260.

Obuku, P.G., and Aki, K., 1987. Fractal geometry in the San Andreas Fault System. J. Geophys. Res. 92, b1:345-355.

Pfeifer, P., 1984. Fractal dimension as a working tool for surface-roughness problems. Applications of Surface Science 18:146-164.

Schmaltz G., 1936. Technische Oberflächenkunde. Berlin: Springer-Verlag.

Turk, N, Grieg, M.G. and Dearman, W.R., 1987. Characterization of rock joint surfaces by fractal dimension. Proc. 28th U.S. Rock Mech. Symp. 1223-1236.

Wright, K. and Karlsson, B., 1982. Fractal analysis and stereological evaluation of microstructures. J. Microscopy 129, pt. 2:185-200.

Voss, R.F., 1988. Fractals in nature: from characterization to simulation. in The science of fractal images. Springer-Verlag, New York.

Zipf, R.K., and Bieniawski, Z.T., 1988. Microscopic studies of fractures generated under mixed mode loading. Proc. 29th U.S. Rock Mech. Symp. 151-158.